Chapter 1 : The Split-Backus Prediction Operator

This chapter presents the theory of the Split-Backus (SB) prediction model. It then examines some real data where seafloor topography is clearly a first order effect in the pegleg multiple arrival times - a fact which few predictive methods in the literature have exploited to date. The chapter goes on to look at a number of statistical procedures for handling the multiple suppression phase of the problem. These methods are not as potentially powerful as the "seafloor-consistent" suppression technique of Chapter 2 but their use may be appropriate when ease of implementation and cost are prime considerations.

1.1 Derivation of Split-Backus Operator

The classical one-dimensional approach to modelling a water-confined reverberation spike train uses the Backus "three-point" operator (Backus,1959). The assumption is that a reverberation filter with Z-transform

$$R(z) = \sum_{i=0}^{\infty}(-cz^n)^i = \frac{1}{1+cz^n} \tag{1.1}$$

operates on the primary response twice prior to observation – once as the source energy passes through the sea-bottom into the sediments and a second time on return to the hydrophones. The reflection coefficient at the sea-bottom is c , ($|c|<1$), and n is the two-way traveltime of the water column in time samples. The filter which cancels these reverberation poles is the three point dereverberation operator

$$\Delta_{Backus} = (1+cz^n)^2 = 1+2cz^n+c^2z^{2n} \tag{1.2}$$

This analysis ignores the fact that both water depth and seafloor reflectivity can depend on shot and geophone locations (Figure 1.1).

The dereverberation operator,

$$\Delta_{Split\ Backus} = (1+c_s z^s)(1+c_g z^g) \tag{1.3}$$

where c_s and c_g are the seafloor reflectivities at the shot and geophone locations, is obtained by a direct extension of the reverberation model. The symbols, z^s and z^g, are the Z-transforms of the vertical water column delays at the shot and at the geophone. The

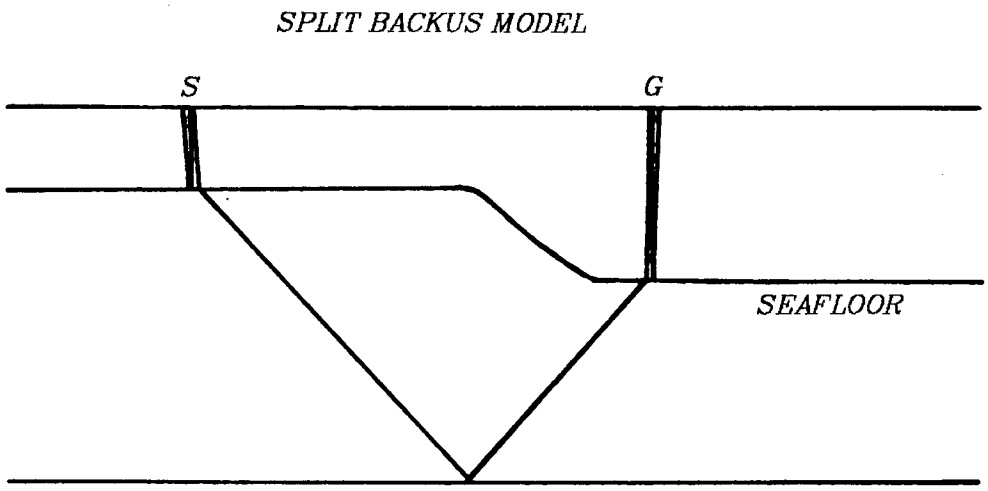

FIG. 1.1. Water depth and seafloor reflectivity as functions of shot and geophone location.

chief approximation here is that the water reverberation paths are indeed nearly vertical (Fig. 1.1). This is a poor approximation for wide-angle water bottom multiples. It is, however, valid for many types of pegleg multiples. The reason the Split Backus (SB) model works where apparently more sophisticated techniques fail is because it recognizes that z^s and z^g may be different.

1.2 Split Peglegs : A Data Example

The next two figures show that split pegleg multiples are an observable phenomenon on real data. Figure 1.2 is a near trace section from a line of offshore Labrador (Flemish Cap) data[1] on which two strong pegleg multiples can be seen cutting across the section between 2.5 and 3.5 seconds.

Figure 1.3 is a constant offset section (COS) from the same line for an offset half-way down the cable (a separation of 45 shot points with this geometry). The first order pegleg multiple starting at 2.5 seconds on the left and running across to 3 seconds on the right is

(1) courtesy of Amoco Canada Ltd.

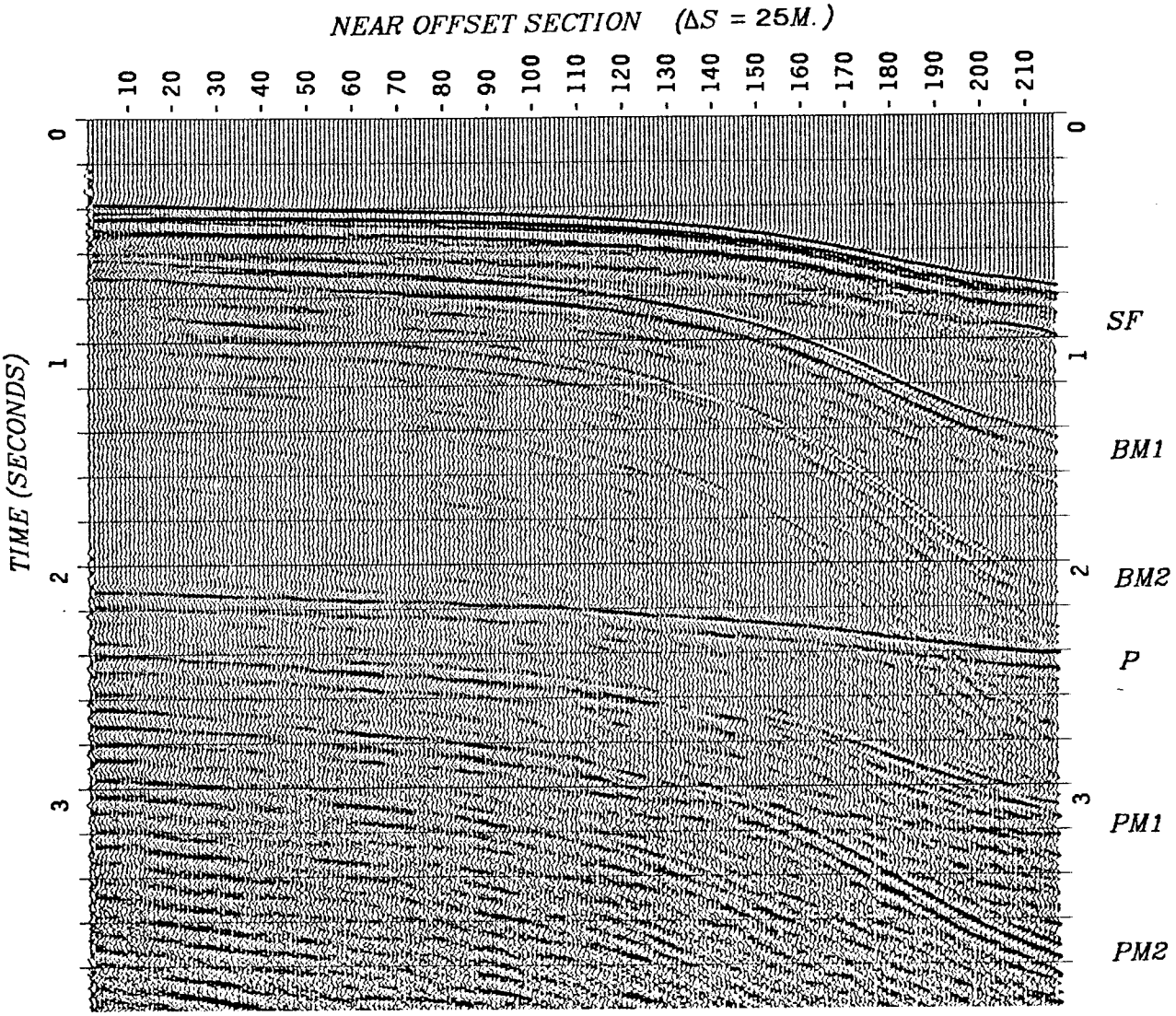

FIG. (1.2). Near Offset Section - offshore Labrador. Offset distance is about 9 shotpoints. Labelled events are SF-seafloor, BM1-first bottom multiple, BM2-second bottom multiple, P-primary, PM1-first pegleg multiple, and PM2-second pegeleg multiple.

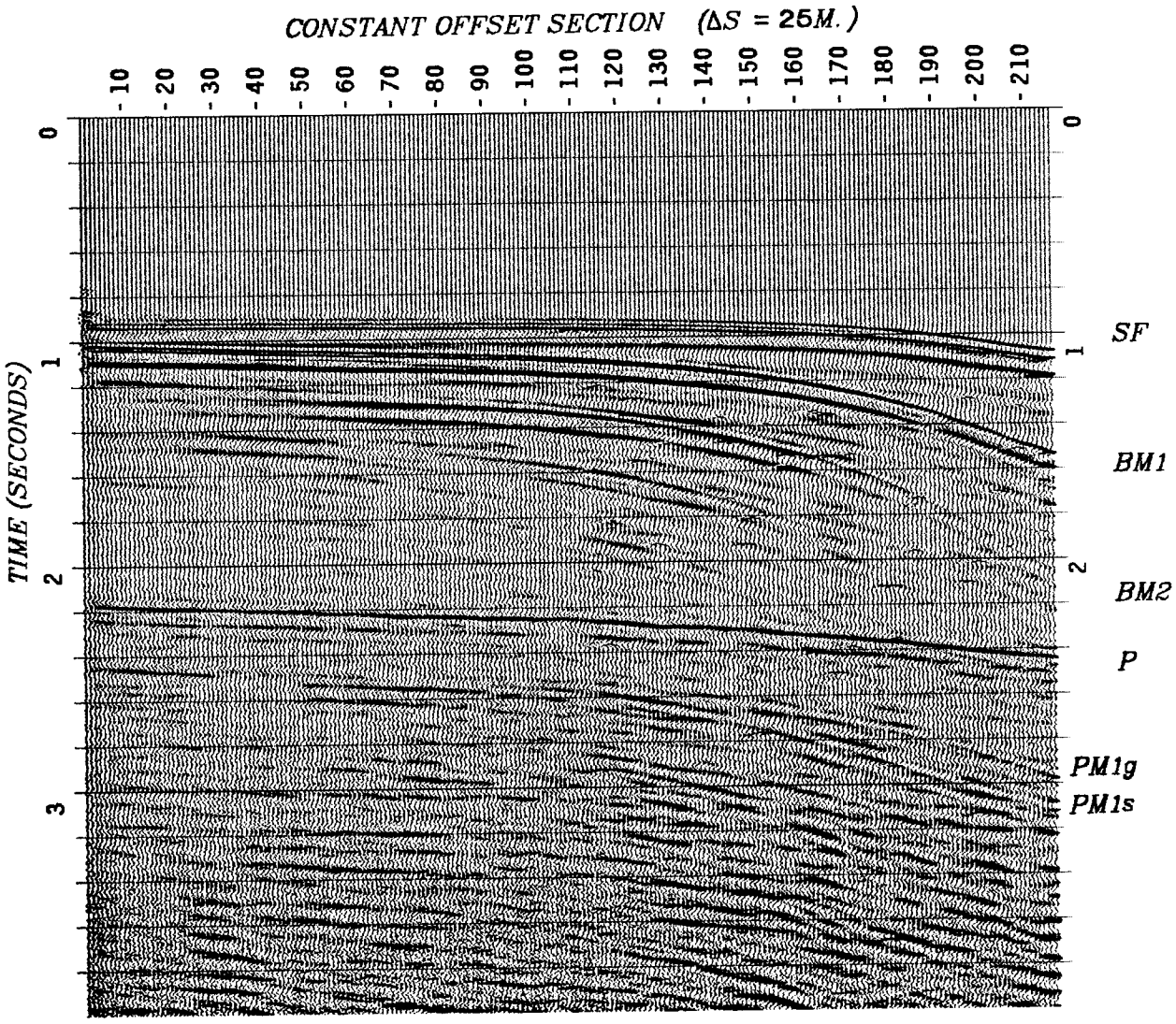

FIG. (1.3). Constant Offset Section (COS) from same line as Fig. 1.2. Offset distance is about 46 shotpoints. Notice that the first order pegleg multiple is now split into two distinct arrivals, $PM1s$ and $PM1g$.

"degenerate" (unsplit) on the near-trace section but is split on the COS due to the seafloor topography. The maximum split is some 200 mils around shot points 180-200. This occurs, as one might expect, where the seafloor has maximum dip; i.e., where the difference between seafloor depths at the shot and geophone positions is greatest.

In order to make an SB prediction, we need to know the water depth at each shot and geophone location along the line. The water depth cannot be obtained from the first break times on the near trace section since there is a substantial gun delay of 100 mils - varying by as much as 15 mils from shot to shot. The autocorrelation of the *near trace section* (Figure 1.4) , however, does provide a good estimate of the seafloor reverberation time as a function of shot location. In Figure 1.4 the seafloor shows up as an event dipping down to the right. The flat events are associated with the shot waveform. The signal/noise ratio of the seafloor event is good enough to automatically track the water depth completely along the line.

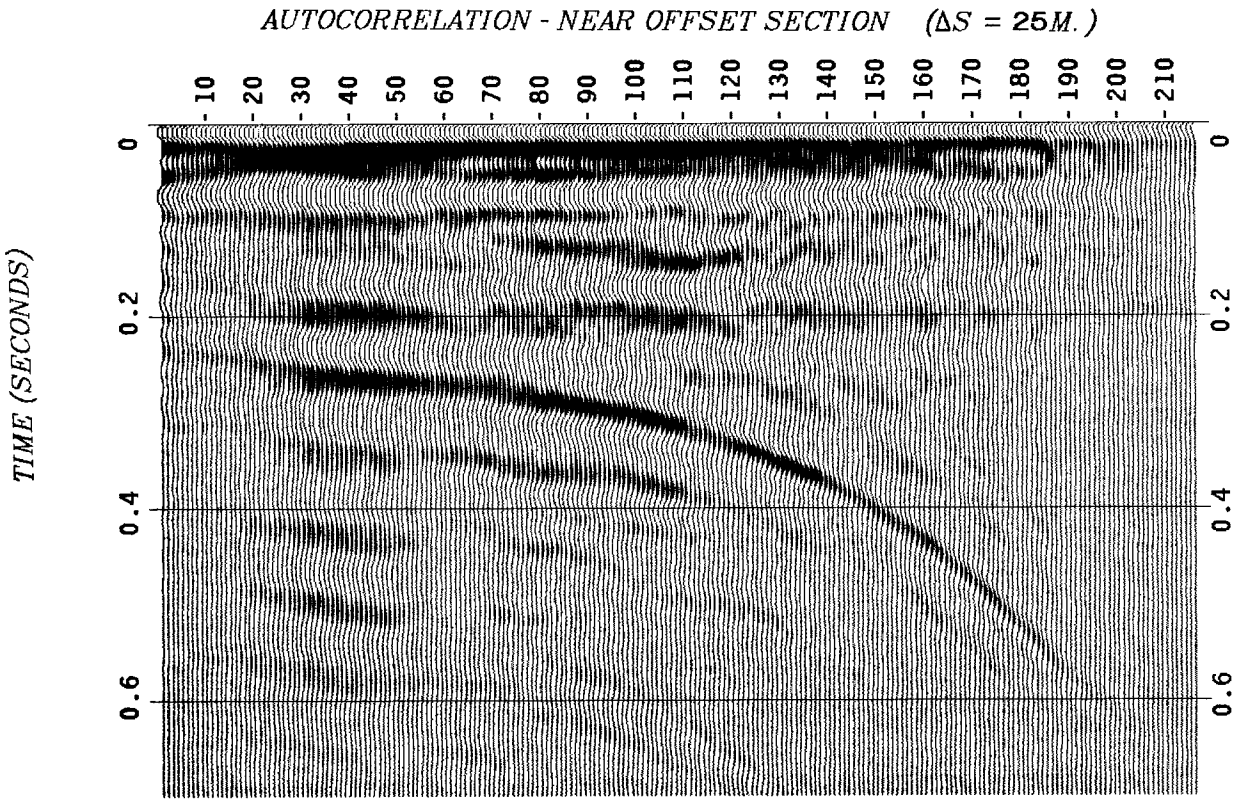

FIG. (1.4). Negative autocorrelation of near trace section. The prominent dipping event gives a good estimate of local seafloor depth.

Figure 1.5 is a pegleg multiple model of the COS of Fig. 1.3 windowed from 2-4 seconds. It was obtained by delaying one copy of the COS by the two-way water time estimate at the shot location, delaying another copy of the COS by the estimated reverberation time 45 shot points down the line (the hydrophone locations), and superposing the two data fields. The low velocity water bottom multiples were removed by dip filter pre-processing. The arrival times of the predicted first-order peglegs match the data peglegs to within a quarter wavelength of the dominant seismic period (i.e.-within 8-10 msec.) across the section. The predicted peglegs consistently precede the data peglegs. This is to be expected since the actual reverberation paths for the constant offset section are at a slight angle to the vertical.

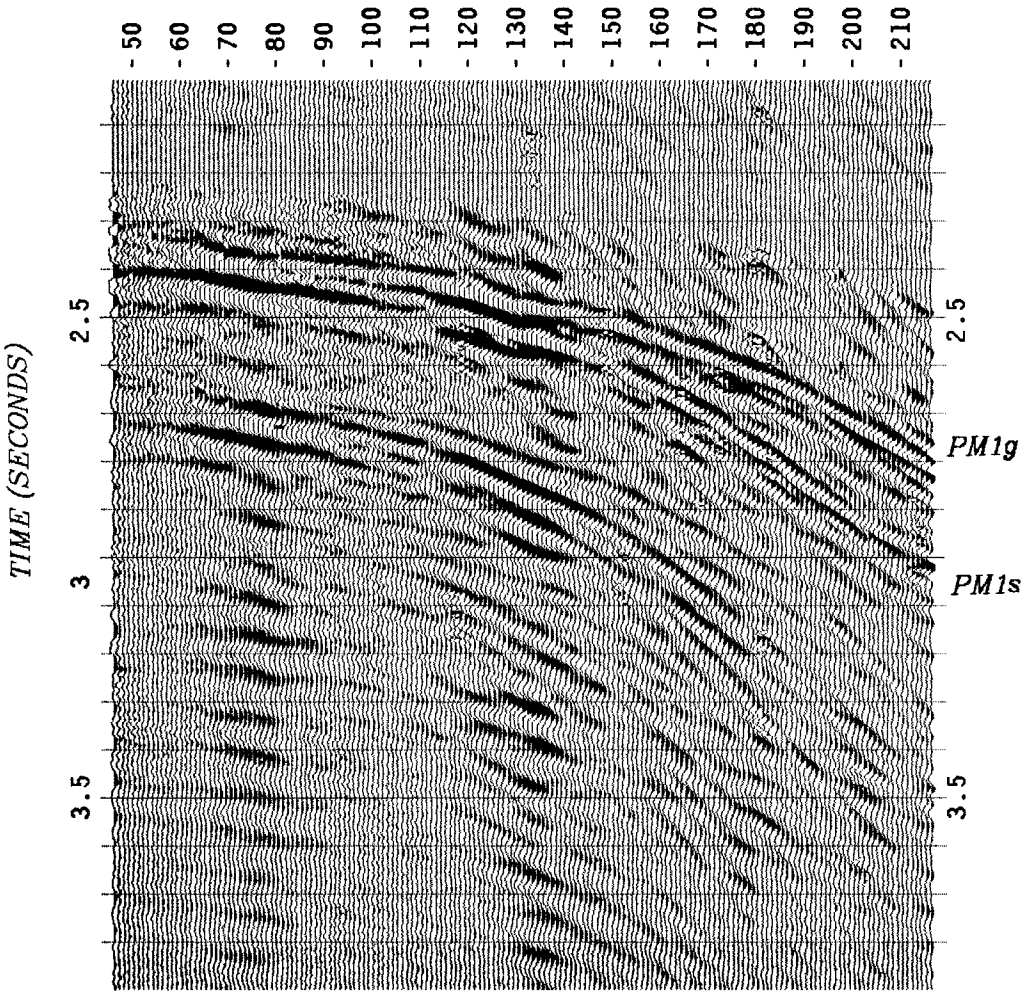

FIG. (1.5). Split-Backus multiple model of constant offset section obtained by superposing two independently delayed copies of Figure 1.3. The delay times are obtained from Figure 1.4. The predicted first order peglegs match the corresponding data peglegs to within one-quarter of the dominant period.

1.3 Estimators for Seafloor Reflectivity

In the general introduction we noted that predictive multiple suppression consisted of two steps - a prediction step and a subtraction or suppression step. Now that we've seen that split pegleg multiples do indeed exist and can be explained by an SB model, we turn our attention to the problem of suppressing these multiples; i.e., estimating the seafloor reflectivity, c. We examine how well three different estimators for the SB deconvolution operator work on the constant offset section of Figure 1.3. In the same way that conventional predictive deconvolution estimates the Backus operator,

$$\Delta_B = (1+cz^n)^2 \tag{1.4}$$

by

$$\hat{\Delta}_B = (1+2\hat{c}z^n) \tag{1.5}$$

all of these estimators will ignore the term in $\hat{c}_s\hat{c}_g$ in the expansion of the SB operator,

$$\Delta_{SB} = (1+c_s z^s)(1+c_g z^g) \tag{1.6}$$

The three estimators we'll examine may be defined by

$$\hat{\Delta}_1 = (1+\hat{c}(z^s+z^g)) \tag{1.7}$$

$$\hat{\Delta}_2 = (1+\hat{c}(t)(z^s+z^g)) \tag{1.8}$$

$$\hat{\Delta}_3 = (1+\hat{c}_s z^s+\hat{c}_g z^g) \tag{1.9}$$

The estimator of equation 1.7 is the solution to the least square shaper filter problem

$$\min E_1 = ||d-\hat{c}*m||^2 \tag{1.10}$$

where d denotes the original data and m, the multiple model ($M(z) = D(z)(z^s+z^g)$). This is equivalent to predictive deconvolution except that the multiple model is now composed of *two*, rather than one, independently time delayed versions of the data. The result, using a 60 msec. filter, is shown in Figure (1.6).

This does a reasonably good job of attenuating the multiple on the left (flat seafloor) side of the section but fails over the dipping-seafloor zone. It unfortunately offers no improvement over a comparable predictive deconvolution - which fails in much the same places (Figure 1.7).

The second estimator (equation 1.8) involved a *weighted* least squares fit of the model to the data. The error norm:

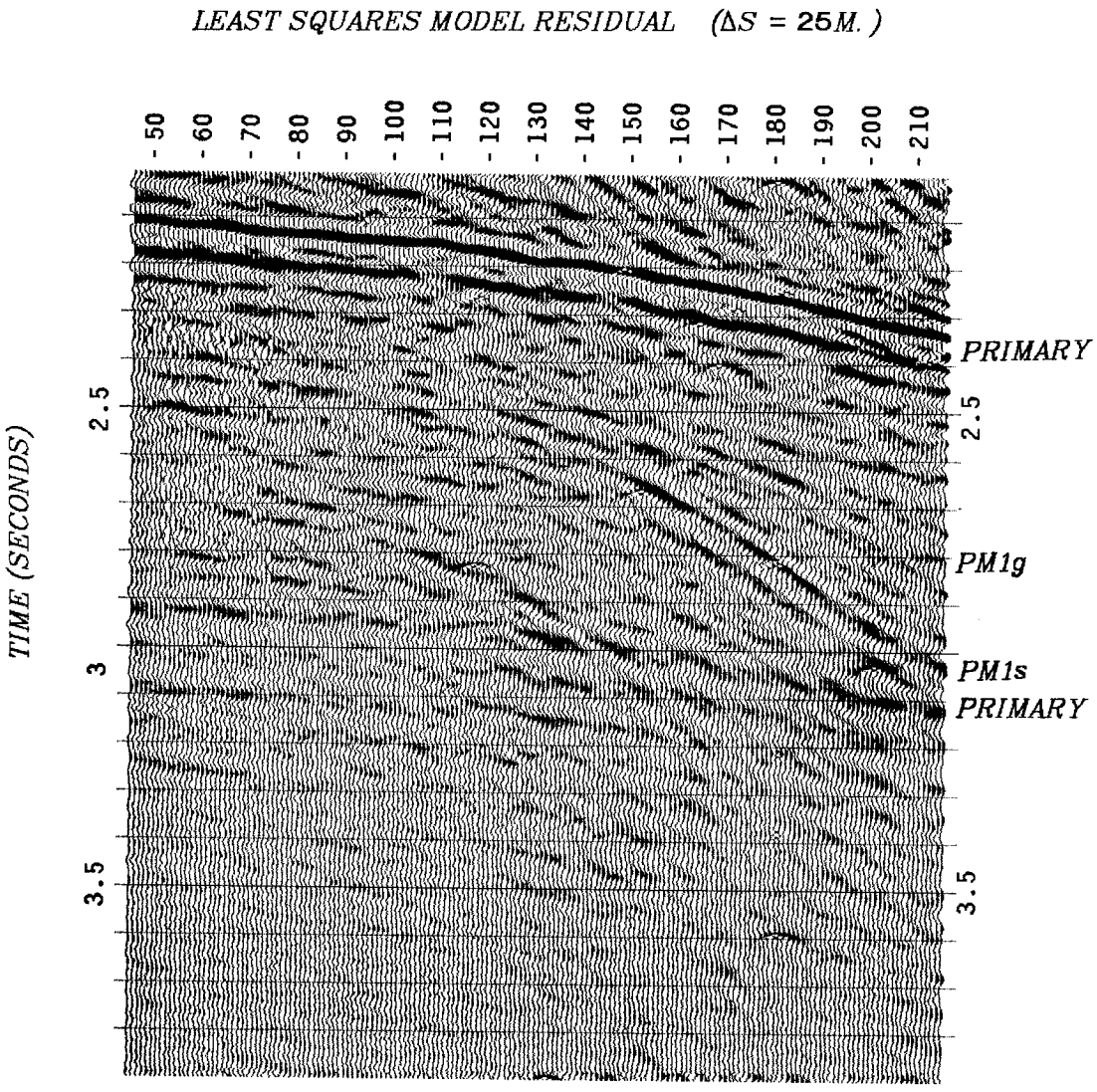

FIG. (1.6). Residual after least square shaper filter fit of Figure 1.5 to Figure 1.3.

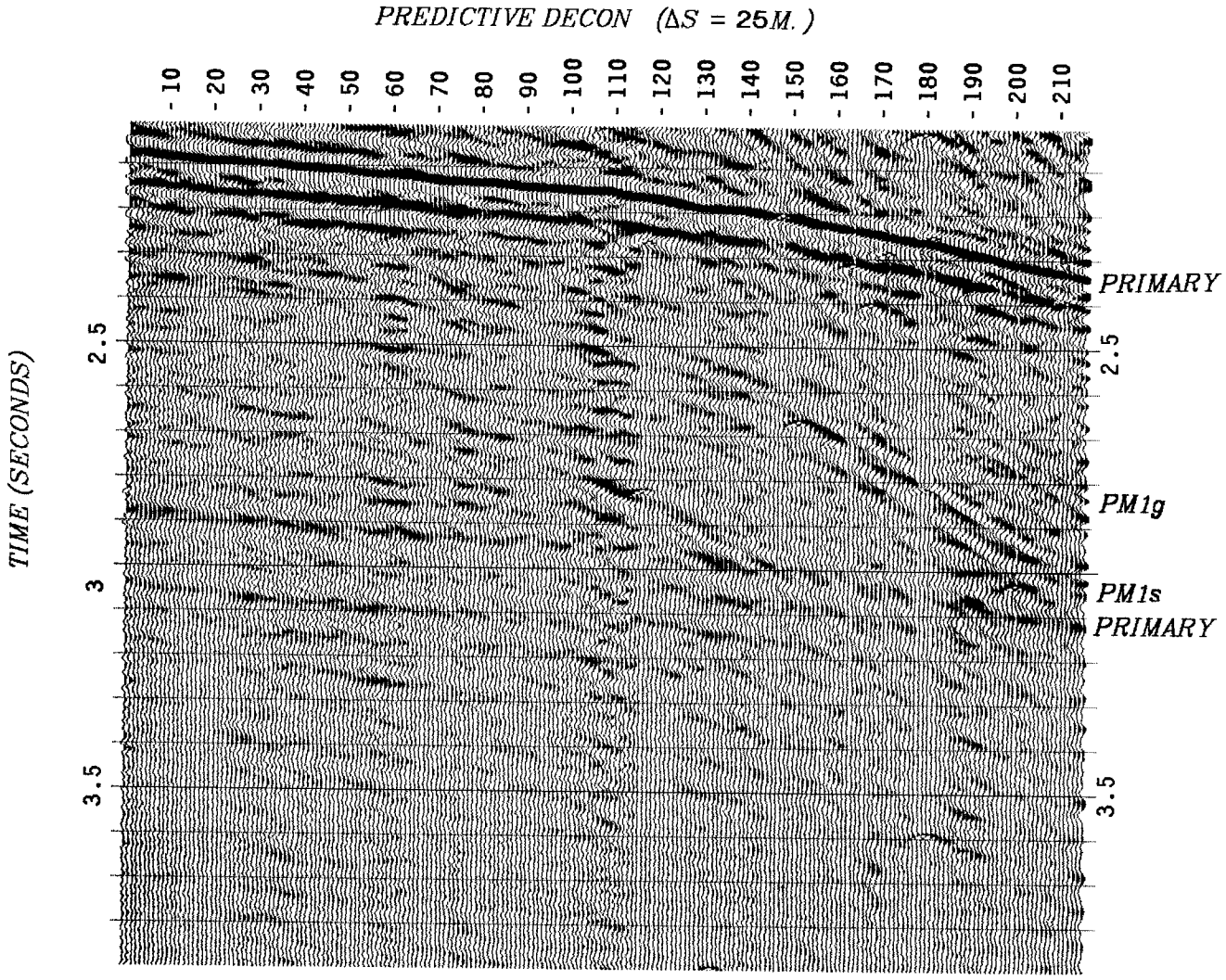

FIG. (1.7). Predictive deconvolution of Figure 1.3. Same filter length as Figure 1.6.

$$E_2 = ||w(d-\hat{c}*m)||^2 \qquad (1.11)$$

was minimized by variation of $\hat{c}$. The required non-Toeplitz matrix inversion was done using Golub's method (Claerbout,'76). The weights, w, were chosen to be the smoothed envelope of the same multiple model, m. The philosophy behind the choice of weights was that the seafloor reflectivity is best estimated by concentrating the filter design on those areas of the data where multiple energy is known to be high. The result is displayed in Figure 1.8.

This filter's overall performance was very similar to that of the unweighted filter. It's relative performance varied widely across the section. In some spots, such as the left side of the dataset, it worked too well - wiping out both primaries and multiples. In other areas it did not appear to do anything. When one considers that this filter's cost is an order of magnitude over the cost of predictive decon, the results were disappointing.

The final statistical model (equation 1.9), and the model which proved to be the best, was a two channel shaper filter. The prediction error,

$$E_3 = ||D-M_s\hat{c}_s-M_g\hat{c}_g||^2 \qquad (1.12)$$

was minimized by simultaneous variation of $\hat{c}_s$ and $\hat{c}_g$.

In equation (1.12) D is the observed seismic trace, $M_s=Dz^s$, or D delayed by the estimated water column reverberation time at the shot location, and $M_g=Dz^g$. The solution of the normal equations for this model (block diagram - Figure 1.9) requires the inversion of a block Toeplitz matrix. Wiggins and Robinson (1965) and Robinson (1967) give an efficient algorithm for this.

This model again ignores the term in $\hat{c}_s\hat{c}_g$ that results from a complete expansion of (2). Thus it does not precisely account for second and higher order pegleg multiples. It is, however, consistent with our general philosophy of attacking the higher amplitude multiples.

Figure (1.10) is the result of applying the process depicted in Figure (1.9) to the same COS example. The primary/multiple ratio is visibly better than the predictive decon result. The split pegleg is well suppressed across the section and the primary around 3 seconds stands out better than after predictive decon (Figure 1.7). This is chiefly because the total number of filter parameters was cut in half. As a bonus, the additional symmetry of the block Toeplitz matrix reduced the computation time significantly over the time of standard predictive deconvolution.

The techniques just described require the user to obtain an estimate of z^s and z^g. In cases where the signal/noise ratio is fairly strong, such estimates can be obtained by automatic picking. If the signal/noise ratio is weaker, however, an unacceptable amount of man-machine interaction may be required to pick z^s and z^g and the methods of the next

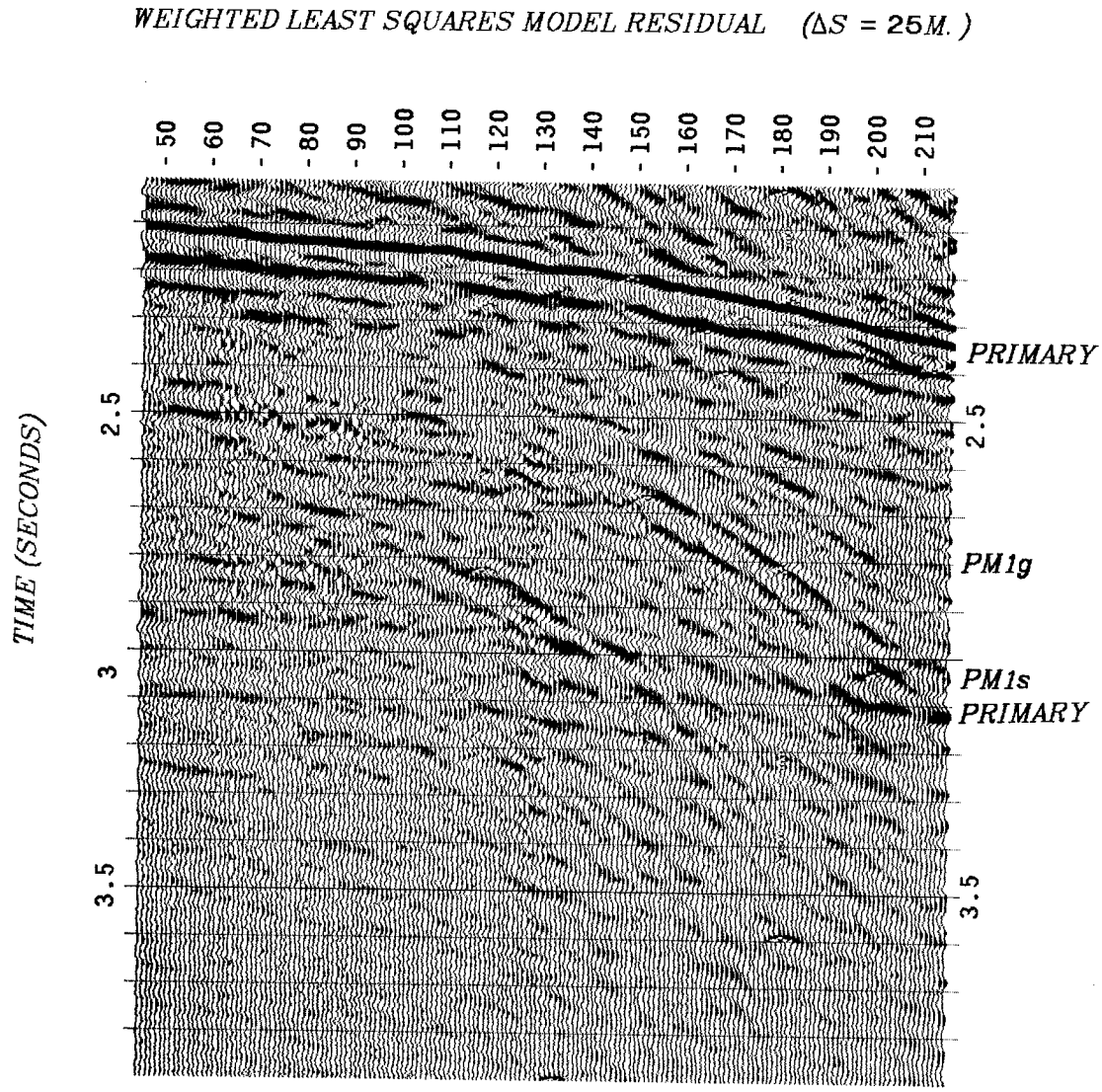

FIG. (1.8). Residual after weighted least-square fit of Figure 1.5 to Figure 1.3.

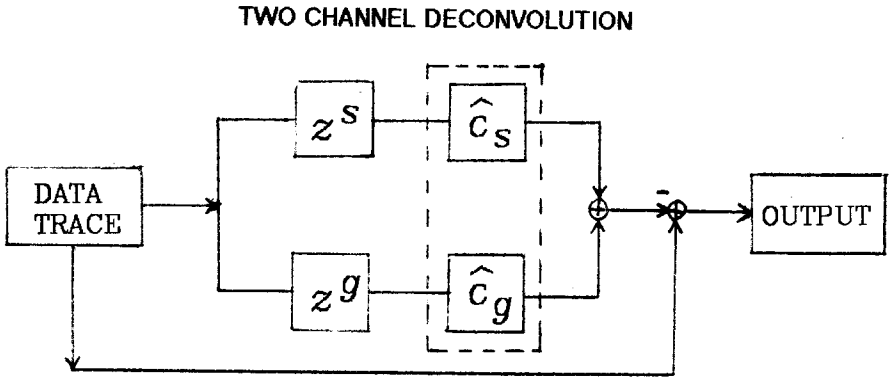

FIG. (1.9). Block diagram for two channel deconvolution of shot and geophone multiples.

chapter become more appropriate.

REFERENCES

Backus, M.M. (1959), Water Reverberations - Their Nature and Elimination, Geophysics 24, pp.233-261.

Claerbout, J.F. (1976), Fundamentals of Geophysical Data Processing, McGraw-Hill

Robinson, E.A. (1967), Multichannel Time Series Analysis, Holden-Day

Wiggins, R.A. and Robinson, E.A. (1965), Recursive Solution to the Multichannel Filtering Problem; J. Geophy. Res., v.70, pp 1885-1891

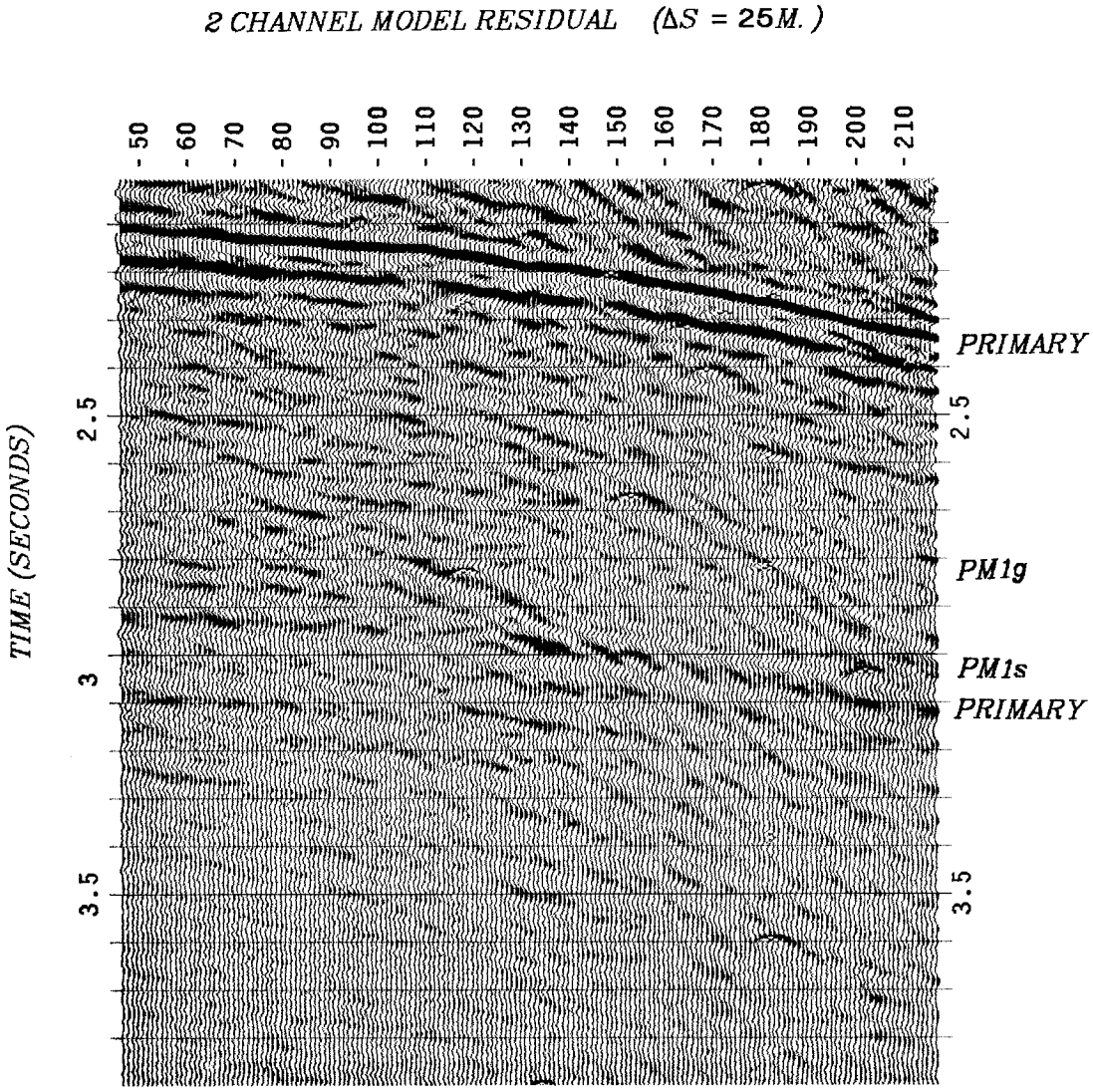

FIG. (1.10). Two channel deconvolution of common offset gather of Figure 1.3. The split pegleg multiple is well suppressed and the primary near 3 seconds comes out better.